



Benzimidazole- and indole-substituted 1,3'-bipyrrolidine benzamides as histamine H₃ receptor antagonists

Derek C. Cole^{a,*}, Jonathan L. Gross^b, Thomas A. Comery^c, Suzan Aschmies^c, Warren D. Hirst^c, Cody Kelley^{c,†}, Ji-In Kim^b, Katie Kubek^c, Xiaoping Ning^{c,‡}, Brian J. Platt^c, Albert J. Robichaud^b, William R. Solvibile^b, Joseph R. Stock^a, Gregory Tawa^b, Marla J. Williams^b, John W. Ellingboe^a

^a Chemical Sciences, Wyeth Research, 401 N. Middletown Rd. Pearl River, NY 10965, United States

^b Chemical Sciences, Wyeth Research, Princeton, NJ 08852, United States

^c Neuroscience, Wyeth Research, Princeton, NJ 08852, United States

ARTICLE INFO

Article history:

Received 19 October 2009

Revised 20 November 2009

Accepted 24 November 2009

Available online 4 December 2009

Keywords:

Histamine H₃ receptor antagonist

Histamine H₃ receptor inverse agonist

ABSTRACT

Using a focused screen of biogenic amine compounds we identified a novel series of H₃R antagonists. A preliminary SAR study led to reduction of MW while increasing binding affinity and potency. Optimization of the physical properties of the series led to (*S*)-**6n**, with improved brain to plasma exposure and efficacy in both water intake and novel object recognition models.

© 2009 Elsevier Ltd. All rights reserved.

Histamine-3 receptors (H₃R) are one of four histamine G-protein coupled receptor subtypes (H_{1–4}R).^{1–3} H₁R and H₂R are post-synaptic receptors involved with allergic responses and gastric acid secretion, respectively, while the H₄R is located on T-cells, neutrophils and monocytes and is implicated in inflammation processes.^{4,5} The H₃R is located presynaptically on histaminergic neurons in the CNS, where it acts as an autoreceptor inhibiting the synthesis and release of histamine. H₃R also acts as a heteroreceptor on non-histaminergic neurons inhibiting the release of other neurotransmitters, including acetylcholine, serotonin, noradrenaline and dopamine. Postmortem studies in humans suggest that decreased brain histamine levels may contribute to the cognitive decline in Alzheimer's disease.⁶ Furthermore H₃R agonists have been shown to impair memory,^{7,8} while H₃R antagonists rescue pharmacologically or genetically induced impairments in various animal models.^{9–13} Based on these findings several H₃R antagonists have advanced to clinical trials for cognitive disorders and dementia.¹⁴

Early H₃R antagonists maintained the histamine imidazole ring, typically connected through an alkyl chain and polar fragment, such as an ether, to a lipophilic moiety (see ciproxifan, **1**¹⁵ and FUB 181, **2**¹⁶ Fig. 1). The presence of the imidazole ring has been

implicated in potential pharmacokinetic liabilities¹⁷ and poor brain penetration, so more recent analogs have focused on imidazole ring replacements, typically with a tertiary amine, (see **3–5**).^{18–20}

Wyeth's H₃R program was initiated with a screen of our focused biogenic amine library using a competitive binding assay²¹ with [³H](*R*)- α -methylhistamine and cell membranes from HEK293T

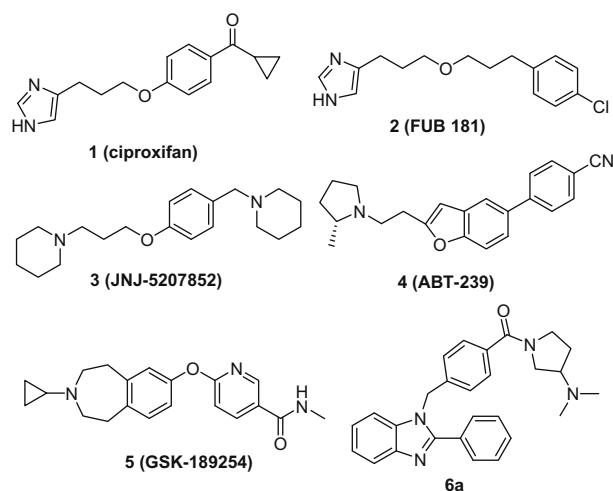


Figure 1. Structures of H₃R antagonists.

* Corresponding author. Tel.: +1 845 602 4619; fax: +1 845 602 5561.

E-mail address: coledc@wyeth.com (D.C. Cole).

[†] Present address: Rutgers University, Newark, NJ 08854, United States.

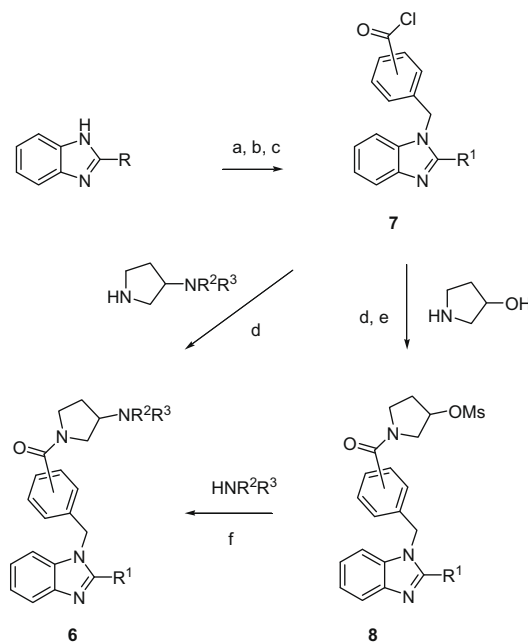
[‡] Present address: J&J Pharmaceutical Research & Development, Titusville, NJ 08560, United States.

cells over-expressing human H_3 receptors (hH_3R) and led to the identification of advanced hit **6a**. This compound had 102 nM binding affinity for hH_3 receptors and was a potent, full antagonist, inhibiting cAMP production in the hH_3 functional assay²² with a K_B value of 11 nM. The compound also showed good overall physicochemical properties with excellent solubility in aqueous buffer ($>100 \mu\text{g/mL}$), good permeability in both PAMPA²³ ($4.4 \times 10^{-6} \text{ cm/s}$) and PAMPA-BBB²⁴ ($9.4 \times 10^{-6} \text{ cm/s}$) assays and passive diffusion in a Caco-2 assay ($P_{A \rightarrow B} = 84.9 \times 10^{-6} \text{ cm/s}$, BA/AB = 1.3) suggesting potentially good absorption, permeability and BBB penetration properties. **6a** also had low inhibition of Cyp450 enzymes and moderate to rapid metabolism in human and rat liver microsomes. However, **6a** has a high molecular weight (424) and $c \log P$ (4.43), resulting in relatively low ligand efficiency (0.3) and high LELP ($c \log P/\text{LE}$) (14.8).²⁵ Therefore, initial efforts were directed at reducing the MW and $c \log P$ of the compounds to more optimal lead-like space, and are described here.

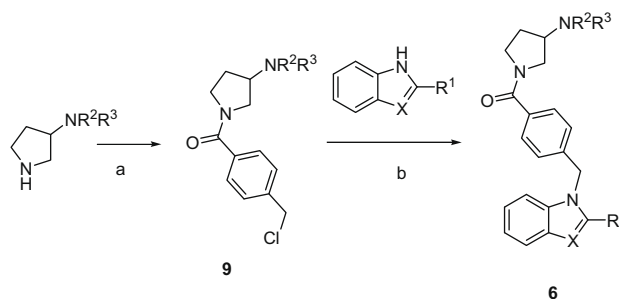
The synthesis of **6a** and related compounds begins with the deprotonation of benzimidazoles followed by coupling with methyl 4-(bromomethyl)benzoate (Scheme 1). Hydrolysis of the ester followed by acid chloride formation generates intermediates **7**, which are coupled with readily available *N,N*-dialkylpyrrolidin-3-amines to afford the desired products **6**. Alternatively, coupling of the acid chlorides with 3-pyrrolidinol followed by mesylate formation leads to intermediate **8**, and displacement with secondary amines gives the desired products **6**. Displacement of the mesylate prepared from (*R*)- or (*S*)-3-pyrrolidinol with inversion of the asymmetric center is used for a stereospecific synthesis of analogs. Initial examination of the connectivity requirement around the central phenyl ring was accomplished using both 2- and 3-(bromomethyl)benzoate (Scheme 1, step a).

To vary the benzimidazole portion of the series, 3-amino substituted pyrrolidines are coupled with 4-chloromethyl benzoyl chloride affording the chloromethyl derivative **9**, which is subsequently reacted with benzimidazoles and indoles to give the desired targets **6** (Scheme 2). The 1,3'-bipyrrolidines **10** are prepared from 3-aminopyrrolidines by *N*-Boc protection of the secondary amine, bis-alkylation of the primary amine and deprotection (Scheme 3).

All of the compounds were evaluated for their ability to displace [^3H](*R*)- α -methylhistamine binding to cloned human H_3 receptors



Scheme 1. Reagents and conditions: (a) NaH, methyl 2-, 3- or 4-(bromomethyl)benzoate, THF/DMF (5:1), rt 16 h; (b) LiOH, MeOH/water (2:1), rt, 16 h; (c) oxalyl chloride (2 M soln. in DCM), DMF (2 drops), DCM rt, 2 h; (d) cyclic amine, DIEA, THF, rt, 2–8 h; (e) Et_3N , MsCl, DCM 0 °C to rt, 16 h; (f) amine, DMF, rt, 16 h.



Scheme 2. Reagents and conditions: (a) DIEA, 4-chloromethyl benzoyl chloride, THF, rt, 2–8 h; (b) NaH, THF/DMF (5:1), rt, 16 h.

Table 1
Binding affinity and functional activity of **6** analogs

Compd	NR^1R^2	R^3	$hH_3 K_i^a$ (nM)	$hH_3 K_b^b$ (nM)
6a	NMe ₂	Ph	100	11
6b	NMeEt	Ph	91	
6c	Pyrrolidine	Ph	10	4
6d	NMeEtOH	Ph	1200	
(<i>S</i>)- 6a	NMe ₂	Ph	65	16
(<i>R</i>)- 6a	NMe ₂	Ph	440	108
6e	NMe ₂	2-pyridyl	235	
6f	NMe ₂	H	390	3
6g	NMe ₂	Me	17	
6h	Pyrrolidine	H	23	
(<i>S</i>)- 6h	Pyrrolidine	H	10	0.5
(<i>R</i>)- 6h	Pyrrolidine	H	27	
(<i>S</i>)- 6i	Pyrrolidine	Me	5	0.3
(<i>R</i>)- 6i	Pyrrolidine	Me	3	2

^a Displacement of [^3H](*R*)- α -methylhistamine binding to cloned hH_3 receptors stably expressed in HEK293T cells.

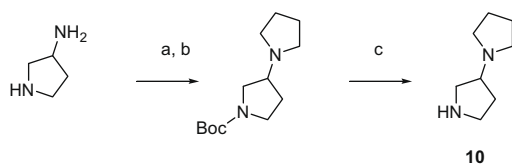
^b Inhibition of cAMP production in HEK293T cells stably transfected with hH_3 receptors. Mean of three determinations with a standard error of $\pm 30\%$.

stably expressed in HEK293T cells. Compounds demonstrating suitable affinity were assayed for inhibition of cAMP production, and shown to be full antagonists. The results are summarized in Tables 1–3.

Variations of the basic amine group (NR^1R^2) present in **6a** led to the identification of the pyrrolidino group (**6c**, Table 1) with a 10-fold improvement in binding affinity. Interestingly, the enantiomeric pairs (e.g., (*R*)- and (*S*)-**6a**) showed only a sevenfold eudismic ratio with respect to both affinity and functional activity in favor of the eutomer (*S*)-**6a**.

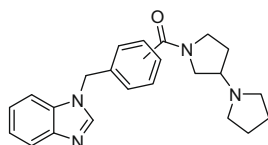
In order to reduce the MW and $c \log P$, a series of analogs were prepared in which the 2-phenyl group in **6a** is replaced with more polar and/or smaller groups. We were gratified to see that indeed this group could be replaced by the 2-pyridyl group (**6e**) with only a slight reduction in potency, whereas replacement with the obviously smaller methyl group (**6g**) provides a significant (sixfold) increase in affinity.

Combining the smaller 2-substituents (i.e., H and Me) with the preferred pyrrolidine tertiary amine leads to **6h–6i**. Again in general the (*S*)-isomer has slightly higher affinity and functional activity than the diastomer with the eutomers exhibiting sub-nanomolar inhibition of cAMP production. Analog **6k** (Table 2) with 1,3 connectivity loses ~ 20 -fold in binding affinity, while the 1,2-con-



Scheme 3. Reagents and conditions: (a) (Boc)₂O, MeOH, rt, 16 h; (b) 1,4-dibromobutane, K₂CO₃, DMF, 110 °C, 16 h; (c) 2 N HCl in dioxane, rt, 3 h.

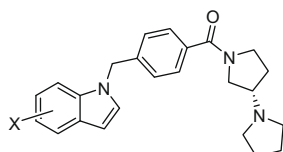
Table 2
Binding affinity of **6** analogs



Compd	Connectivity	hH ₃ K _i (nM)
6h	1,4	23
6k	1,3	400
6l	1,2	4000

Displacement of [³H]-(R)-α-methylhistamine binding to cloned hH₃ receptors stably expressed in HEK293T cells. Mean of three determinations with a standard error of ±30%.

Table 3
Binding affinity and functional activity of **6** analogs



Compd	X	hH ₃ K _i (nM)	hH ₃ K _b (nM)
(S)- 6m	H	15	2.4
(S)- 6n	7-Cl	2.5	0.3
(S)- 6o	6-Cl	150	2.1
(S)- 6p	5-Cl	130	0.9

Displacement of [³H]-(R)-α-methylhistamine binding to cloned hH₃ receptors stably expressed in HEK293T cells. Mean of three determinations with a standard error of ±30%.

nected analog **6l** is nearly 200-fold less potent, showing a strict requirement for the 1,4 substitution pattern among these ligands.

The pharmacokinetic profile of (S)-**6h** in rats indicates high clearance, moderate volume of distribution and half-life and excellent bioavailability (Table 4). Brain and plasma exposure measured after a 10 mg/kg ip injection show AUCs of 231 and 1039 h ng/mL respectively, indicating a brain to plasma ratio of 0.22. The low brain exposure is somewhat surprising given the low MW, *c log P* and polar surface area (PSA) of (S)-**6h** (see Table 5).^{26,27}

Replacing the benzimidazole with an indole ((S)-**6m**) and chloro-substituted indoles ((S)-**6n–p**) results in compounds which are calculated to have a slightly higher log *P* and lower PSA. While the solubility of these analogs is slightly reduced the permeability in both PAMPA and PAMPA–BBB is improved significantly, suggesting potentially improved brain to plasma ratios. The unsubstituted indole analog (S)-**6m** demonstrates comparable activity to the corresponding benzimidazole ((S)-**6h**) however the 7-chloro derivative (S)-**6n** has sixfold increased affinity and functional activity at the hH₃R (Table 3).

Unfortunately, the rat pharmacokinetic profile of (S)-**6n** shows rapid clearance, low exposure and oral bioavailability (Table 4).

Table 4
Pharmacokinetic properties for (S)-**6h** and (S)-**6n** in rats

	(S)- 6h	(S)- 6n
iv dose (mg/kg)	2	2
Clp (mL/min/kg)	56	112
Vss (L/kg)	3.6	7.3
po dose (mg/kg)	10	10
C _{max} (ng/mL)	1751	22
T _{max} (h)	0.4	1.2
AUC (h ng/mL)	2736	63
t _{1/2}	1.3	1.9
F%	93	5
ip dose (mg/kg)	10	30
C _{max} brain/plasma (b/p) (ng/mL)	92/388	6536/1086
C _{max} brain (nM)	245	16019
%Fu (brain)	13.8	3.5
T _{max} b/p (h)	1.0/1.0	0.5/0.5
AUC b/p (h ng/mL)	231/1039	15007/2182
b/p ratio	0.2	6.9

Table 5
Calculated and measured properties of selected **6** analogs

Compd	MW	<i>c log P</i>	<i>p log D</i>	PSA ^a	Pe ^b	BBB ^c	aq sol. ^d
6a	424.5	4.2	3.4	41.3	4.4	9.4	>100
(S)- 6h	374.5	2.6	1.4	41.4	0.3	3.7	51
(S)- 6i	388.5	2.9	1.6	41.4	0.3	4.0	32
(S)- 6m	373.5	3.6	2.3	28.5	8.3	9.4	28
(S)- 6n	407.9	4.4	3.0	28.5	6.5	7.0	18
(S)- 6o	407.9	4.4	3.0	28.5	7.3	8.6	13
(S)- 6p	407.9	4.4	3.0	28.5	7.8	8.1	10

^a PSA = polar surface area.

^b Pe = effective permeability measured by PAMPA method (×10^{−6} cm/s).²³

^c BBB = blood–brain barrier permeability measured by PAMPA–BBB method (×10^{−6} cm/s).²⁴

^d Aqueous solubility μg/mL at pH 3.1.

However, the brain and plasma exposure measured after a 30 mg/kg ip injection in rats shows a significant improvement with AUCs of 15007 and 2182 h ng/mL for brain and plasma, respectively, and a brain to plasma ratio of 6.9. The fraction of (S)-**6n** unbound in brain is 3.5%, giving a free drug concentration of 229 ng/mL or 562 nM at T_{max}, approximately 25-fold greater than the rH₃ affinity (rH₃ K_i = 21.7 nM). Compound (S)-**6n** demonstrates >1000-fold selectivity for hH₃R over hH₁R and hH₂R receptors and >100-fold selectivity over various serotonin (5-HT_{2a,2c,6,7}), dopamine (D₂) and alpha adrenergic (α_{1,2a}) receptors in binding assays.

The selective H₃R agonist (R)-α-methylhistamine has been shown to induce a dose dependent increase in water consumption in rats mediated by H₃R within the CNS.^{28,29} This increased water intake effect was blocked by (S)-**6n** dosed intraperitoneally (ip) at both 10 and 30 mg/kg (Fig. 2).

Furthermore, H₃R antagonists have been shown to reverse delay-dependent deficits in rodent novel object recognition by enhancing memory encoding and/or retention.^{30,31} In the novel object recognition model, rats previously exposed to identical objects can discriminate between a novel object and a familiar, previously experienced object, during a subsequent trial. Figure 3 shows a statistically significant differential exploration of the novel and familiar object for rats dosed with (S)-**6n** (minimally efficacious dose = 0.3 mg/kg) prior to the learning trial. The preferential exploration of the novel object demonstrates enhanced object recognition memory in rats dosed with (S)-**6n** relative to those dosed with vehicle and represents efficacy as a cognitive enhancer.

In summary, we have identified a potent and selective series of H₃R antagonists. Optimization led to analogs with increased

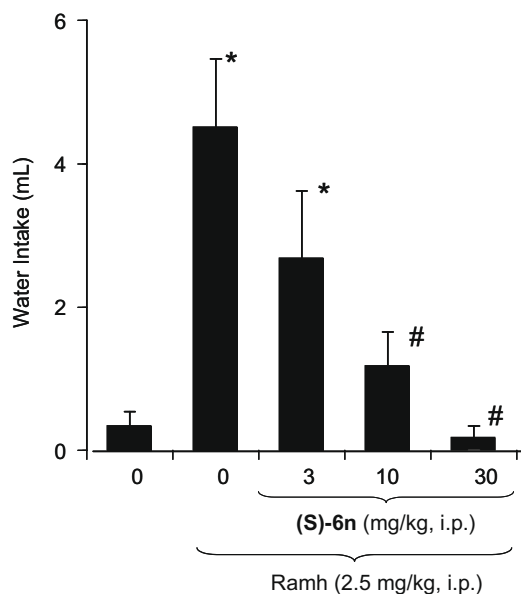


Figure 2. Effect of (S)-6n on (R)- α -methylhistamine (Ramh)-induced water consumption in rats. * p <0.05 versus veh; # p <0.05 versus Ramh alone.

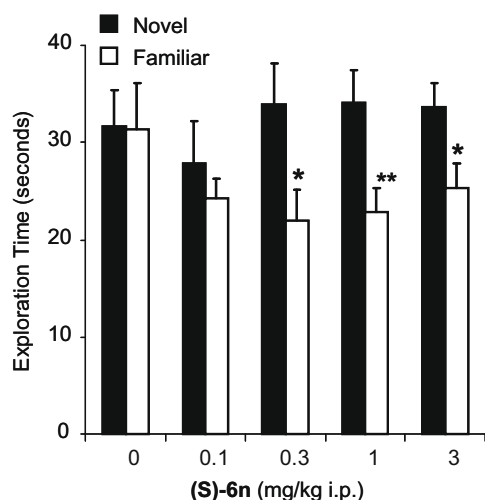


Figure 3. Novel object recognition in rats after ip dosing of the H₃R antagonist (S)-6n. * p <0.03; ** p <0.005.

affinity and potency, and further modulation of the physical properties of the series led to (S)-6n, which has excellent brain to plasma exposure and demonstrated efficacy in both the water intake and novel object recognition rat models.

Acknowledgments

We thank Christine Huselton, Jonathan Schantz, William Adams and Adedayo Adedoyin for providing PK data.

References and notes

1. Arrang, J. M.; Garbarg, M.; Schwartz, J. C. *Nature* **1983**, 302, 832.

2. Lovenberg, T. W.; Roland, B. L.; Wilson, S. J.; Jiang, X.; Pyati, J.; Huvar, A.; Jackson, M. R.; Erlander, M. G. *Mol. Pharmacol.* **1999**, 55, 1101.
3. Hough, L. B. *Mol. Pharmacol.* **2001**, 59, 415.
4. Hill, S. J.; Ganellin, C. R.; Timmerman, H.; Schwartz, J. C.; Shankley, N. P.; Young, J. M.; Schunack, W.; Levi, R.; Haas, H. L. *Pharmacol. Rev.* **1997**, 49, 253.
5. Hofstra, C. L.; Desai, P. J.; Thurmond, R. L.; Fung-Leung, W. P. *J. Pharmacol. Exp. Ther.* **2003**, 305, 1212.
6. Panula, P.; Rinne, J.; Kuokkanen, K.; Eriksson, K. S.; Sallmen, T.; Kalimo, H.; Relja, M. *Neuroscience* **1998**, 82, 993.
7. Blandina, P.; Giorgetti, M.; Bartolini, L.; Cecchi, M.; Timmerman, H.; Leurs, R.; Pepeu, G.; Giovannini, M. G. *Br. J. Pharmacol.* **1996**, 119, 1656.
8. Prast, H.; Argyriou, A.; Philippu, A. *Brain Res.* **1996**, 734, 316.
9. Miyazaki, S.; Onodera, K.; Imaizumi, M.; Timmerman, H. *Life Sci.* **1997**, 61, 355.
10. Meguro, K.; Yanai, K.; Sakai, N.; Sakurai, E.; Maeyama, K.; Sasaki, H.; Watanabe, T. *Pharmacol. Biochem. Behav.* **1995**, 50, 321.
11. Fox, G. B.; Pan, J. B.; Esbenshade, T. A.; Bennani, Y. L.; Black, L. A.; Faghih, R.; Hancock, A. A.; Decker, M. W. *Behav. Brain Res.* **2002**, 131, 151.
12. Komater, V. A.; Browman, K. E.; Curzon, P.; Hancock, A. A.; Decker, M. W.; Fox, G. B. *Psychopharmacology (Berl.)* **2003**, 167, 363.
13. Komater, V. A.; Buckley, M. J.; Browman, K. E.; Pan, J. B.; Hancock, A. A.; Decker, M. W.; Fox, G. B. *Behav. Brain Res.* **2005**, 159, 295.
14. Celanire, S.; Wajtmans, M.; Talaga, P.; Leurs, R.; de Esch, I. J. *Drug Discovery Today* **2005**, 10, 1613.
15. Esbenshade, T. A.; Krueger, K. M.; Miller, T. R.; Kang, C. H.; Denny, L. I.; Witte, D. G.; Yao, B. B.; Fox, G. B.; Faghih, R.; Bennani, Y. L.; Williams, M.; Hancock, A. A. *J. Pharmacol. Exp. Ther.* **2003**, 305, 887.
16. Stark, H.; Huls, A.; Ligneau, X.; Purand, K.; Pertz, H.; Arrang, J. M.; Schwartz, J. C.; Schunack, W. *Arch. Pharm. (Weinheim)* **1998**, 331, 211.
17. Yang, R.; Hey, J. A.; Aslanian, R.; Rizzo, C. A. *Pharmacology* **2002**, 66, 128.
18. Apodaca, R.; Dvorak, C. A.; Xiao, W.; Barbier, A. J.; Boggs, J. D.; Wilson, S. J.; Lovenberg, T. W.; Carruthers, N. I. *J. Med. Chem.* **2003**, 46, 3938.
19. Cowart, M.; Pratt, J. K.; Stewart, A. O.; Bennani, Y. L.; Esbenshade, T. A.; Hancock, A. A. *Bioorg. Med. Chem. Lett.* **2004**, 14, 689.
20. Heightman, T. D. WO2004035544, 2004.
21. HEK293T cells expressing the human cloned histamine H₃ receptor were harvested in phosphate-buffered saline (PBS) and pelleted by centrifugation at 1000g for 5 min at 4 °C and membranes were prepared by homogenizing the cell pellets in ice-cold 50 mM Tris–HCl buffer, pH 7.4 and 0.5 mM EDTA for approximately 30 s using a Polytron homogenizer. The homogenates were centrifuged at 40,000g for 30 min at 4 °C, and the resulting pellet was re-homogenized and centrifuged as described above. The membranes were finally resuspended in 50 mM Tris–HCl buffer, pH 7.4 at a concentration of approximately 1 mg protein/mL, and were stored at –70 °C until use. Receptor binding studies were carried out on these membranes in 50 mM Tris–HCl buffer, pH 7.4, at room temperature. Assays consisted of 100 μ L of displacing compound (final concentration of 0.05 nM–500 nM) or buffer, 20 μ L of [³H]R- α -methylhistamine at a final concentration of 5 nM and the reaction was initiated by the addition of 100 μ L of human H₃ receptor membranes (30 μ g of protein/well). Nonspecific binding was determined in the presence of 10 mM clobenpropit. The experiments were terminated by rapid filtration through a GF/B filter plate (presoaked in 0.1% (v/v) polyethyleneimine), and then the filters were washed with ice-cold buffer (50 mM Tris–HCl). Filters were dried and then 25 μ L of Microscint 20 was added to each well. Radioactivity was determined by liquid scintillation spectrometry using a Packard TopCount.
22. Functional in vitro activity of the compounds was determined in cAMP accumulation assays. Culture media was removed from the cells and they were washed twice with PBS (Ca²⁺/Mg²⁺-free) containing 500 μ M IBMX. Cells were detached, by gentle tapping, and resuspended in the same buffer. 2000 cells/well were incubated with 1 μ M histamine, 10 μ M forskolin and test compounds (0.03 nM–10 μ M) in a total volume of 30 μ L in 96-well plates for 30 min at 30 °C. Cyclic AMP levels were then measured using the HitHunter cAMP kit (DiscoverX, Fremont, CA) according to the manufacturer's instructions. Chemiluminescent signals were detected using a Packard TopCount. Data were analyzed using Prism.
23. Kerns, E. H.; Di, L. *Drug Discovery Today* **2003**, 8, 316.
24. Di, L.; Kerns, E. H.; Fan, K.; McConnell, O. J.; Carter, G. T. *Eur. J. Med. Chem.* **2003**, 38, 223.
25. Keseru, G. M.; Makara, G. M. *Nat. Rev. Drug Disc.* **2009**, 8, 203.
26. Clark, D. E. *Drug Discovery Today* **2003**, 927.
27. Lobell, M.; Molnar, L.; Keseru, G. M. *J. Pharm. Sci.* **2003**, 92, 360.
28. Clapham, J.; Kilpatrick, G. J. *Eur. J. Pharmacol.* **1993**, 232, 99.
29. Kraly, F. S.; Tribuzio, R. A.; Kim, Y. M.; Keefe, M. E.; Finkell, J. *Physiol. Behav.* **1995**, 58, 1091.
30. Blandina, P.; Giorgetti, M.; Cecchi, M.; Leurs, R.; Timmerman, H.; Giovannini, M. G. *Inflamm. Res.* **1996**, 45, S54.
31. Pascoli, V.; Boer-Saccomani, C.; Hermant, J. F. *Psychopharmacology (Berl)* **2009**, 202, 141.